Astron. Astrophys. 360, L43–L46 (2000)

ASTRONOMY AND ASTROPHYSICS

LETTER

Letter to the Editor

Reconstruction of radial temperature profiles of galaxy clusters

Y.-J. Xue and X.-P. Wu

Chinese Academy of Sciences, Beijing Astronomical Observatory and National Astronomical Observatories, Beijing 100012, P.R. China

Received 27 June 2000 / Accepted 26 July 2000

Abstract. In this Letter we present the radial temperature profiles of three X-ray clusters (A119, A2255 and A2256) reconstructed from a combination of the X-ray surface brightness measurements and the universal density profile as the underlying dark matter distribution. Our algorithm is based on the hydrostatic equilibrium for intracluster gas and the universality of the total baryon fraction within the virial radius. The scaled temperature profiles of these three clusters appear to be remarkably similar in shape, reflecting the underlying structural regularity, although they are inconsistent with either isothermality or a significant decline with increasing radius. Nevertheless, we find a good agreement between our derived temperature profiles and the recent analysis of 11 clusters observed with BeppoSAX (Irwin & Bregman 2000), which provides a useful clue to resolving the temperature profile discrepancy raised recently in literature. A comparison of our derived temperature profiles with future spatially-resolved spectral measurements may constitute a critical test for the standard model of structure formation and the conventional scenario for dynamical properties of clusters.

Key words: cosmology: dark matter — galaxies: clusters: general — X-rays: galaxies

1. Introduction

The lack of robust constraints on the radial temperature profiles of hot gas contained within galaxy clusters is probably the major uncertainty in the present determination of dynamical properties of clusters, which hinders clusters from acting as an ideal laboratory of testing theories of formation and evolution of structures in the universe including a direct estimate of the cosmic mass density parameter $\Omega_{\rm M}$ by combining the baryon fraction measurement and the Big Bang Nucleosynthesis. Indeed, previous studies have arrived at conflicting results regarding the radial temperature gradients in clusters. By analyzing 30 clusters observed with ASCA, Markevitch et al. (1998) claimed a significant temperature decline with radius quantified by a polytropic index of 1.2-1.3 on the average. However, subsequent studies have soon raised doubt about the ubiquity and steepness of these temperature decline: Irwin, Bregman & Evrard (1999) carried out an analysis of the color profiles of the same clusters used by Markevitch et al. (1998) but found an essentially flat temperature profile. Applying the spectral-imaging deconvolution method to a large sample of 106 ASCA clusters, White (2000) has showed that 90 percent of the temperature profiles are actually consistent with isothermality. Further argument against the nonisothermality of intracluster gas has been put forward recently by Irwin & Bregman (2000), who reported the detection of a flat and even increasing temperature profile out to $\sim 30\%$ of the viral radius for a sample of 11 clusters observed with BeppoSAX.

Theoretically, it deserves an investigation into the possibility of deriving the radial temperature profiles of intracluster gas from the well-motivated physical mechanisms, incorporated with the X-ray imaging observations. This may provide a valuable clue to resolving the above temperature profile discrepancy. There are two well-established facts on which we can rely today: (1)The gravitational potential of a cluster is dominated by the dark matter distribution which can be described by the so-called universal density profile, as suggested by a number of high-resolution simulations (Navarro, Frenk & White 1995 and hereafter NFW), although the innermost slope is still under debate. (2)The azimuthally-averaged X-ray surface brightness of a cluster is reliably measurable out to several or even ~ 10 times as large as the X-ray core radius, for which a good approximation is provided by the conventional β model (Cavaliere & Fusco-Femiano 1976). These two facts, along with the hydrostatic equilibrium hypothesis and a reasonable choice of the boundary conditions, permit a unique determination of the gas temperature profile (Wu & Chiueh 2000). On the other hand, a comparison of the theoretically expected temperature profile with the result from the X-ray spectroscopic measurement constitutes a critical test for the validity of the NFW profile and the hydrostatic equilibrium in clusters.

In this Letter, we will attempt for the first time to derive the temperature profiles of 3 well-defined clusters with good X-ray imaging observations extending to relatively large radii, based on the method developed by Wu & Chiueh (2000). Our derived temperature profiles will be compared with the recent results of 11 clusters observed with BeppoSAX (Irwin & Bregman 2000).

Send offprint requests to: Y.-J. Xue
Correspondence to: wxp@class1.bao.ac.cn

We will examine the possible similarity in the gas temperature profiles as a result of the underlying structural regularity (e.g. Neumann & Arnaud 1999). The implication of our results for the reported temperature profile discrepancy will be discussed. Throughout the Letter we assume $H_0 = 50$ km s^{-1} Mpc^{-1} and a flat cosmological model with $\Omega_{\rm M} = 0.3$ and $\Omega_\Lambda = 0.7$.

2. Theoretical expectations

We briefly summarize the mathematical treatment of the intracluster gas tracing the underlying dark matter distribution of clusters. First, if the X-ray surface brightness profile of a cluster can be well approximated by the conventional β model (Cavaliere & Fusco-Femiano 1976)

$$S_{\rm x}(r) = S_0\left(1+\frac{r^2}{r_{\rm c}^2}\right)^{-3\beta+1/2}, \qquad (1)$$

this would indicate (Cowie, Henriksen & Mushotzky 1987),

$$n_{\rm e}(r)T^{1/4}(r) = n_{\rm e0}T_0^{1/4}\left(1+\frac{r^2}{r_{\rm c}^2}\right)^{-3\beta/2} \qquad (2)$$

for an optically-thin, thermal bremsstrahlung emission, where $n_{\rm e}$ and T are the electron number density and temperature, respectively. The central electron number density $n_{\rm e0}$, temperature T_0 and X-ray surface brightness S_0 are connected by

$$n_{\rm e0}^2 = \frac{4\pi^{1/2}}{\alpha(T_0)\mu_{\rm e} g}\frac{\Gamma(3\beta)}{\Gamma(3\beta-1/2)}\frac{S_0(1+z)^4}{r_c}, \qquad (3)$$

where $\alpha(T_0) = (2^4e^6/3m_{\rm e}\hbar c^2)(2\pi kT_0/3m_{\rm e}c^2)^{1/2}$, $\mu_{\rm e} = 2/(1+X)$ with X being the primordial hydrogen mass fraction, $g \approx 1.2$ is the average Gaunt factor, and z is the cluster redshift. The total mass in gas within r is simply

$$M_{\rm gas}(r) = 4\pi\mu_{\rm e}m_p n_{\rm e0}\int\left(\frac{T_0}{T}\right)^{1/4}\left(1+\frac{r^2}{r_{\rm c}^2}\right)^{-3\beta/2} r^2 dr. \qquad (4)$$

Secondly, if the intracluster gas is in hydrostatic equilibrium with the underlying dark matter distribution, we have

$$\frac{GM_{\rm DM}(r)}{r^2} = -\frac{1}{\mu m_{\rm p} n_{\rm e}}\frac{d(n_{\rm e}kT)}{dr}. \qquad (5)$$

where $\mu = 0.585$ is the average molecular weight. For NFW profile

$$M_{\rm DM}(r) = 4\pi\rho_{\rm s}r_{\rm s}^3\left[\ln\left(1+\frac{r}{r_{\rm s}}\right) - \frac{r}{r+r_{\rm s}}\right]. \qquad (6)$$

Here we have neglected the self-gravity of the gas. Using the normalized gas temperature $\tilde{T}(r) \equiv T(r)/T_0$ and the volume-averaged baryon fraction $f_{\rm b}(r) \equiv M_{\rm gas}(r)/M_{\rm DM}(r)$ as the two variables, we obtain the following two first-order differential equations

$$\frac{d\tilde{T}}{dx} = \frac{4\beta x\tilde{T}}{x^2+a^2} - \frac{4\alpha_0}{3x^2}\left[\ln(1+x) - \frac{x}{1+x}\right]; \qquad (7)$$

$$\frac{df_{\rm b}}{dx} = \frac{b\tilde{T}^{-1/4}(1+x^2/a^2)^{-3\beta/2}x^2 - f_{\rm b}x/(1+x)^2}{\ln(1+x) - x/(1+x)}, \qquad (8)$$

where $x = r/r_{\rm s}$, $a = r_{\rm c}/r_{\rm s}$, $b = \mu_{\rm e}n_{\rm e0}m_{\rm p}/\rho_{\rm s}$ and $\alpha_0 = 4\pi G\mu m_{\rm p}\rho_{\rm s}r_{\rm s}^2/kT_0$. The first equation can be straightforwardly solved with $\tilde{T}(0) = 1$:

$$\tilde{T}(x) = \left(1+\frac{x^2}{a^2}\right)^{2\beta}\left[1 - \frac{4\alpha_0}{3}\int_0^x \frac{\ln(1+x) - x/(1+x)}{x^2(1+x^2/a^2)^{2\beta}}dx\right]. \qquad (9)$$

In order to solve the second equation and determine the free parameters a, b and α_0, we use the following boundary conditions

$$f_{\rm b}(r_{\rm vir}) = f_{\rm b,BBN}; \qquad (10)$$

$$\frac{df_{\rm b}}{dx}\Big|_{x=r_{\rm vir}/r_{\rm s}} = 0. \qquad (11)$$

Namely, we demand that the baryon fraction should asymptotically match the universal value of $f_{\rm b,BBN}$ at the virial radius $r_{\rm vir}$ defined by

$$M_{\rm DM}(r_{\rm vir}) = \frac{4\pi}{3}r_{\rm vir}^3\Delta_{\rm c}\rho_{\rm crit}, \qquad (12)$$

where $\Delta_{\rm c}$ represents the overdensity of dark matter with respect to the average background value $\rho_{\rm crit}$, for which we take $\Delta_{\rm c} = 178\Omega_{\rm M}^{0.45}(z)$ and $\Omega_{\rm M}(z) = \Omega_{\rm M}(1+z)/\{1+z\Omega_{\rm M} + [(1+z)^{-2} - 1]\Omega_\Lambda\}$. We now come to the free parameters involved in Eqs. (8) and (9). With the X-ray imaging observation, we can obtain the best-fit values of β, $r_{\rm c}$ and S_0. If, on the other hand, the X-ray spectroscopic measurement can set a useful constraint on the central temperature T_0, we will be able to derive the central electron density from Eq. (3). As a result, there are only two free parameters in the above equations: $\rho_{\rm s}$ (or equivalently $\delta_{\rm c} = \rho_{\rm s}/\rho_{\rm crit}$) and $r_{\rm s}$. These two parameters can be fixed during the numerical searches for the solution of Eqs. (8) and (9) using the boundary conditions Eqs. (10) and (11). This will allow us to work out simultaneously the radial profiles of gas density and temperature, and fix the dark matter (NFW) profile of the cluster characterized by $\rho_{\rm s}$ and $r_{\rm s}$.

3. Application to X-ray clusters

Since the reconstruction of gas temperature profile is sensitive to the initial input of $S_{\rm x}$ especially the β parameter, whether or not we can reliably derive the temperature profile depends critically on the goodness of the single β model fit to the X-ray surface brightness profile. We thus restrict ourselves to the X-ray flux-limited sample of 45 clusters published recently by Mohr, Mathiesen & Evrard (1999), in which there are sufficiently large data points to set robust constraints on the β model fit. The inclusion of a cluster is based on the following two criteria: (1)The X-ray surface brightness profile can be well fitted by a single β model with $0.8 \leq \chi_\nu^2 \leq 1.25$; (2)The maximum extension ($r_{\rm m}$) of the X-ray observed surface brightness profile should be large enough to guarantee the validity of the β model at the outermost regions of clusters. Here we set $r_{\rm m} \geq 1.5$ Mpc. Unfortunately, it turns out that there are only three clusters which meet our criteria (Table 1): A119, A2255 and A2256. In fact, our first criterion implies that the effect of cooling flows in the central

Table 1. Cluster sample

cluster	A119	A2255	A2256
z	0.0438	0.0808	0.0581
T_0 (keV)	5.80	7.30	7.51
S_0^*	1.18	1.68	4.41
β	0.662	0.792	0.828
$r_{\rm c}$ (Mpc)	0.494	0.608	0.500
$n_{\rm e0}$ (10^{-3}cm^{-3})	1.37	1.67	2.94
b	4.15	3.48	3.31
α_0	17.80(12.30)$^+$	14.66(24.80)$^+$	13.15(13.21)$^+$
$\delta_{\rm c}$	130(490)$^+$	184(230)$^+$	345(1220)$^+$
$r_{\rm s}$ (Mpc)	5.77(2.59)$^+$	4.82(5.99)$^+$	3.43(2.03)$^+$

*In units of 10^{-13} erg s^{-1} cm^{-2} arcmin^{-2} for energy band 0.5-2.0 keV;
$^+$The result for an isothermal gas distribution.

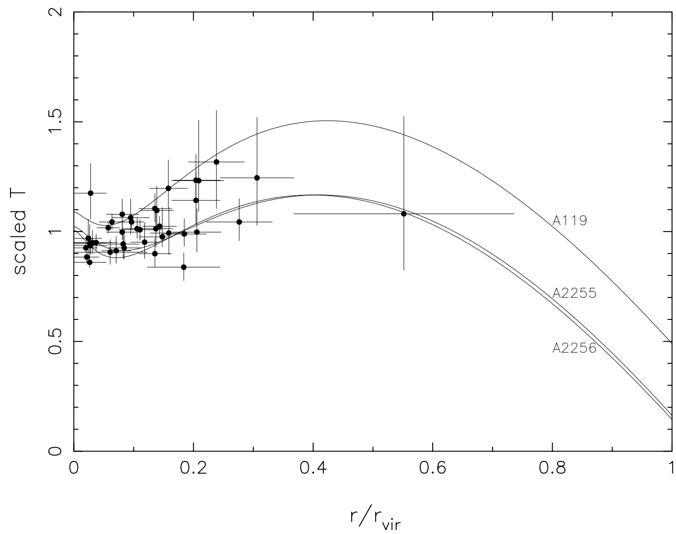

Fig. 1. A comparison of the derived radial temperature profiles of three clusters (A119, A2255 and A2256) with the results of 11 clusters observed with BeppoSAX (Irwin & Bregman 2000). The observed data are normalized by the mean temperature for each cluster, while the derived temperature curves are scaled by $1.32T_0$ for comparison. The horizontal axis is in units of the virial radius.

regions of clusters should be negligibly small. This explains the fact that the three selected clusters all have large core radii. Note that the presence of cooling flows may lead to the failure of a single β model fit to the X-ray surface brightness profiles. In other words, our method cannot be applied to the clusters with strong cooling flows. While the X-ray imaging data of the clusters can be somewhat accurately acquired, the present X-ray spectral measurements have yielded the emission-weighted temperatures rather than the central values T_0 appearing in the α_0 parameter. Therefore, we have to use the emission-weighted temperature as a first approximation of T_0. Alternatively, we adopt the universal baryon fraction $f_{\rm b,BBN} = 1/6$ to reconcile our cosmological model of $\Omega_{\rm M} = 0.3$ (for $\Omega_{\rm b} = 0.05$).

Using the available X-ray data of the three clusters from Mohr et al. (1999), we have performed numerical searches for the solutions of Eqs. (8) and (9) by iterations until the boundary conditions Eqs. (10) and (11) are satisfied. The resulting parameters α_0, $\delta_{\rm c}$ and $r_{\rm s}$ are summarized in Table 1, together with a comparison with the corresponding values for an isothermal gas distribution estimated in previous work (Wu & Xue 2000). Most importantly, such a procedure enables us to completely fix the radial profiles of gas density, temperature and baryon fraction for the three clusters. Here we have no intention to illustrate the radial variations of $n_{\rm e}(r)$ and $f_{\rm b}(r)$, which essentially follow the theoretical expectations (Wu & Chiueh 2000). Rather, we display in Fig. 1 the radial profiles of the emission-weighted temperatures for the three clusters constructed from our algorithm. Surprisingly, none of the temperature profiles of these three clusters are consistent with the conventional speculations, and a visual examination of Fig. 1 reveals that they are neither characterized by isothermality nor represented simply by the polytropic equation of state. Nevertheless, these temperature profiles indeed demonstrate a similar radial variation, reflecting probably the underlying structural regularity. Basically, the radial variation of the gas temperature resembles a distorted 'S' in shape: There exist two turnover points roughly at $0.1r_{\rm vir}$ and $0.4r_{\rm vir}$, respectively, where $dT/dr = 0$, which separate the temperature curve $T(r)$ into three parts – a decreasing $T(r)$ with radius inside the cluster core of $\sim 0.1r_{\rm vir}$, following a slightly increasing $T(r)$ until $\sim 0.4r_{\rm vir}$, and finally a moderately decreasing $T(r)$ out to the virial radius. Overall, the absolute values of the gas temperature do not demonstrate a dramatic change within clusters.

The azimuthally-averaged radial temperature profiles of 11 clusters derived by Irwin & Bregman (2000) from an analysis of the BeppoSAX data are superimposed on Fig. 1. It appears that our derived temperature profiles are in good agreement with their observed ones over entire radius range. In fact, the significant temperature discrepancy raised in different X-ray spectral measurements occurs in the inner parts of clusters. In the outer regions, it seems that many observations have provided a moderately decreasing temperature profile, which is essentially consistent with our theoretical predictions. Alternatively, our result is also compatible with the gas temperature distribution at large radii revealed by numerical simulations that demonstrate a temperature decline of $\sim 30\%$ of the central value at the virial radius (Frenk et al. 1999).

4. Discussion and conclusions

In the absence of the detailed information on the radial temperature profiles of clusters from X-ray spectroscopic measurements, we have made an attempt to derive the gas temperature profiles by combining the X-ray surface brightness measurements and the NFW profile as the underlying dark matter distribution of clusters. This has become possible when the intracluster gas is required to satisfy the hydrostatic equilibrium and the volume-averaged baryon fraction within the viral radius is required to asymptotically match the universal value. Consequently, we have obtained semi-analytically the temperature profiles of three clusters selected carefully from the ROSAT observed cluster sample. These derived temperature profiles are consistent with the new observations of 11 BeppoSAX clusters (Irwin & Bregman 2000) and other measurements made at large cluster radii (e.g. Markevitch et al. 1998) as well as the result given by numerical simulations (e.g. Frenk et al. 1999).

Regardless of the small sample, the three clusters exhibit a temperature profile similar in shape when the length scales are normalized to their virial radii, perhaps indicative of the underlying structural regularity. The present study provides a helpful clue to resolving the temperature profile discrepancy: It is very likely that the lack of the high-quality data of the spatially resolved spectral observations would yield an emission-weighted temperature roughly close to isothermality within $\sim 80\%$ of the virial radius, which does not exclude the possibility that a slightly increasing temperature profile may be marginally detectable in the range of $0.1r_{\rm vir} < r < 0.4r_{\rm vir}$. This explains the recent observations of Irwin & Bregman (2000) and other studies (e.g. Kikuchi et al. 1999; White 2000; etc.). However, our model does not predict the flat temperature profile toward the inner regions of clusters as reported particularly by Markevitch et al. (1998), although a moderately decreasing temperature profile will ultimately take place in the outer clusters ($r > 0.4r_{\rm vir}$).

A conclusive test for the universality of our derived temperature profiles can be provided by future X-ray spectroscopic measurements. Indeed, it will be useful to apply the present method to other X-ray clusters with good X-ray surface brightness profiles measured to large radii and high-quality data of the spatially-resolved spectral observations at least within the central regions. This may allow us to further justify our model and include the measurement uncertainties which have been neglected in the present study. The inconsistency of the predicted temperature profiles with the X-ray spectroscopic results will challenge the prevailing models of structure formations as well as the conventional scenario of cluster dynamics such as the hydrostatic equilibrium. Finally, we should point out that our proposed method to obtain the temperature profiles of clusters can be significantly contaminated by nongravitational heating processes especially from the supernova-driven protogalactic winds. Recall that the asymptotic tendency of the derived temperature profiles at large radii depends sensitively on the β parameter, while the energy injection of supernovae and active galaxies into the intracluster gas will result in a shallower X-ray surface brightness distribution (David et al. 1990; Ponman, Cannon & Navarro 1999; Llyod-Davies, Ponman & Cannon 2000). Without correction to this effect the theoretically predicted temperature profiles may rise too rapidly at large radii. Note that at large radii the NFW mass profile diverges logarithmically with r, which differs significantly from the variation of the gas mass profile (roughly $M_{\rm gas} \propto r$) expected from the assumption of isothermality. For a cluster with smaller β, $r_{\rm c}$ and $r_{\rm s}$, an increasing temperature profile near virial radius is thus required to maintain the universality of the cluster baryon fraction. Therefore, a robust, theoretical determination of the temperature profiles of clusters should also allow nongravitational heating processes to be included.

Acknowledgements. We gratefully acknowledge Tzihong Chiueh for useful discussion and comments, and an anonymous referee for valuable suggestions. This work was supported by the National Science Foundation of China, under Grant 19725311.

References

Cavaliere A., Fusco-Femiano R., 1976, A&A, 49, 137
Cowie L. L., Henriksen M., Mushotzky R. F., 1987, ApJ, 317, 593
David L. P., Arnaud K. A., Forman W., Jones C., 1990, ApJ, 356, 32
Frenk C. S., et al., 1999, ApJ, 525, 554
Irwin J. A., Bregman J. N., 2000, ApJ, in press
Irwin J. A., Bregman J. N., Evrard A. E., 1999, ApJ, 519, 518
Kikuchi K., et al., 1999, PASJ, 51, 301
Lloyd-Davies E. J., Ponman T. J., Cannon D. B., 2000, MNRAS, in press
Markevitch M., Vikhlinin A., Forman W. R., Sarazin C. L., 1998, ApJ, 527, 545
Mohr J. J., Mathiesen B., Evrard A. E., 1999, ApJ, 517, 627
Navarro J. F., Frenk C. S., White S. D. M., 1995, MNRAS, 275, 720 (NFW)
Neumann D. M., Arnaud M., 1999, A&A, 348, 711
Ponman T. J., Cannon D. B., Navarro J. F., 1999, Nature, 397, 135
White D. A., 2000, MNRAS, 312, 663
Wu X.-P., Chiueh T., 2000, ApJ, in press
Wu X.-P, Xue, Y.-J., 2000, ApJ, 529, L5